Journal of the European Ceramic Society 17 (1997) 1639–1645

PII: S0955-2219(96)00018-6
0955-2219/97/$17.00

On the Extension of the α-Sialon Phase Area in Yttrium and Rare-Earth Doped Systems

Zhijian Shen[a] & Mats Nygren[b]

[a]Department of Materials Sci. and Eng., Zhejiang University, Hangzhou 310027, P. R. China
[b]Department of Inorganic Chemistry, Arrhenius Laboratory, Stockholm University, S-106 91 Stockholm, Sweden

(Received 18 November 1996; accepted 3 January 1997)

Abstract

The extension of the α-sialon phase area in Y, Yb, Dy and Nd doped sialon systems has been mapped out on the basis of element analysis of individual α-sialon grains. The α-sialon-forming area expands with decreasing size of the M ion in $M_xSi_{12-(m+n)}Al_{m+n}O_nN_{16-n}$. *The maximum* n *value,* n_{max} *is ~1·0 for M = Nd and ~1·2 for the other dopants. The* m *value varies from ~1·0 in all systems studied to a value of 2·75 in the Yb–α-sialon system, indicating that the substitution of Al–O units for Si–N in α-sialon is more restricted than substitution of Al–N for Si–N. It is shown that the lattice expansion of the α-sialon phase with increasing content of M ions is due to the substitution of Al–N units for Si–N, while the lattice parameters are not at all or only very slightly dependent on the ionic radius of the M ion. Based on the elemental analysis of individual α-sialon grains and the lattice parameters obtained, the following empirical relation between the sizes of the* a *and* c *axes and the* m *and* n *values of the α-sialon phase was obtained:*

$$a(Å) = 7{\cdot}752 + 0{\cdot}036\ m + 0{\cdot}02\ n$$
$$c(Å) = 5{\cdot}620 + 0{\cdot}031\ m + 0{\cdot}04\ n$$

1 Introduction

In a number of articles by the present authors and others the thermal stability of the α-sialon phase has been studied. The general conclusion of all these studies seems to be that the α-phase is stable at high temperatures ($T \geq 1750$°C), but once formed it decomposes when exposed to post-heat-treatment in the temperature region $1350 \leq T \leq 1750$°C. The rate of decomposition is seemingly dependent on the ionic size of M, i.e. the Nd α-sialon phase decomposes faster than its Y and Yb analogues. The decomposition pathways of the α-sialon phase in the different sialon systems have been mapped out in some detail. In order to be able to understand why these reactions occur, and to be able to understand why the thermal stability of α-sialon phase is different in different sialon systems, we need detailed information of the extensions of the α-sialon-forming regions at elevated temperatures ($T \geq 1750$°C). In addition, knowledge of the oxygen/aluminium-rich boundary of the α-sialon phase area facing the β-sialon phase is of technical importance. It is well known that many physical properties of sialon-based ceramics depend on the amount and kind of grain boundary phase(s) present in the final compact. In order to be able to prepare α/β-sialon ceramics with a minimum of grain boundary phase(s) we need a profound knowledge of the oxygen/aluminium-rich boundary of the α-sialon phase area facing the β-sialon phase.

The phase relationships between α-sialon and other phases in the M–Si–Al–O–N systems with M = Y, Yb, Dy, Sm and Nd, and the compositional limits of the α phase, $M_xSi_{12-(m+n)}Al_{m+n}O_nN_{16-n}$, along the join line Si_3N_4–M_2O_3 * 9 AlN for the same M elements, have recently been reported in some detail.[1–9] Detailed knowledge of the extension of the two-dimensional phase region of α-sialon, i.e. maximum m and n values in the formula above, is available for Y- and Sm-sialon systems, but there is still some uncertainty concerning the maximum value of n in the Y-sialon system. Stutz *et al.*[7] have suggested a value of 1·24, while Sun *et al.*[8] report n_{max} to be 1·7. An n_{max} value of ~1·2 was found in the Sm-sialon system.[9] This article presents the extensions of the α-sialon phase areas at 1750°C in Nd-, Dy-, Yb- and Y- sialon systems.

Hampshire *et al.*[10,11] have derived empirical relationships between cell dimensions and the m, n values and the size of the M ion in $M_xSi_{12-(m+n)}Al_{m+n}O_nN_{16-n}$. Sun *et al.*[8] derived similar relationships, but came to the conclusion that

the cell parameters were not dependent on the M ion size but merely on the m and n values. As shown below, our data seem to support the findings of Sun *et al.*,[8] but we obtain a slightly different relation between the lattice parameters and m and n.

2 Experimental procedure

Powders of Si_3N_4 (UBE, SN-10E), AlN (HC Starck-Berlin, grade A), Y_2O_3 (HC Starck-Berlin, grade finest) and R_2O_3 (R = Nd, Dy, and Yb, Johnson Matthey Chemicals Ltd, 99·9%) were

Table 1. Starting mixtures (wt%), k value and overall composition formulae

Nd System						
Sample	Si_3N_4	*AlN*	Al_2O_3	Nd_2O_3	*Overall formula*	k
ANd02	88·05	6·56	0	5·39	$Nd_{0.20}Si_{11.679}Al_{0.995}O_{0.824}N_{16.218}$	0·744
ANd035	79·88	10·83	0	9·29	$Nd_{0.35}Si_{10.758}Al_{1.668}O_{1.025}N_{15.678}$	0·744
ANd04	77·3	12·2	0	10·5	$Nd_{0.40}Si_{10.527}Al_{1.900}O_{1.095}N_{15.605}$	0·744
ANd06	67·42	17·34	0	15·24	$Nd_{0.60}Si_{9.488}Al_{2.790}O_{1.371}N_{15.127}$	0·744
ANd07	63·05	19·65	0	17·83	$Nd_{0.70}Si_{8.849}Al_{3.153}O_{1.502}N_{14.650}$	0·743
ANd08	58·39	22·05	0	19·56	$Nd_{0.80}Si_{8.537}Al_{3.686}O_{1.651}N_{14.768}$	0·744
ANd02-13	80·5	10·8	3·05	5·69	$Nd_{0.20}Si_{10.115}Al_{1.555}O_{0.775}N_{14.725}$	0·753
ANd035-17	71·14	15·26	4·02	9·63	$Nd_{0.35}Si_{9.243}Al_{2.272}O_{0.981}N_{14.291}$	0·754
ANd035-13	74·25	14·43	1·73	9·63	$Nd_{0.35}Si_{9.647}Al_{2.146}O_{0.991}N_{14.697}$	0·752
ANd048-13	69·18	17·41	0·64	12·82	$Nd_{0.48}Si_{8.993}Al_{2.588}O_{1.180}N_{14.704}$	0·729
Dy System						
Sample	Si_3N_4	*AlN*	Al_2O_3	Dy_2O_3	*Overall formula*	k
ADy02	87·14	6·6	0	6·36	$Dy_{0.2}Si_{10.861}Al_{0.926}O_{0.787}N_{15.083}$	0·743
ADy025	85·13	7·71	0	7·76	$Dy_{0.25}Si_{10.871}Al_{1.126}O_{0.867}N_{15.295}$	0·742
ADy035	79·03	10·72	0	10·25	$Dy_{0.35}Si_{10.696}Al_{1.659}O_{1.022}N_{15.589}$	0·744
ADy04	76·3	12·1	0	11·6	$Dy_{0.4}Si_{10.428}Al_{1.891}O_{1.091}N_{15.468}$	0·744
ADy06	66·28	17·05	0	16·67	$Dy_{0.6}Si_{9.456}Al_{2.781}O_{1.370}N_{15.076}$	0·744
ADy07	61·53	19·18	0	19·29	$Dy_{0.7}Si_{8.850}Al_{3.154}O_{1.502}N_{14.653}$	0·743
ADy08	57·16	21·57	0	21·27	$Dy_{0.8}Si_{8.521}Al_{3.677}O_{1.925}N_{14.738}$	0·744
ADy10	48·91	25·69	0	25·84	$Dy_{1.0}Si_{7.502}Al_{4.506}O_{0.787}N_{14.225}$	0·743
ADy02-13	80	10·72	3·03	6·28	$Dy_{0.2}Si_{10.098}Al_{1.551}O_{0.774}N_{14.699}$	0·753
ADy035-17	70·4	15·09	3·99	10·56	$Dy_{0.35}Si_{9.248}Al_{2.271}O_{0.981}N_{14.299}$	0·754
ADy035-13	73·48	14·3	1·7	10·56	$Dy_{0.35}Si_{9.653}Al_{2.150}O_{0.992}N_{14.710}$	0·752
ADy048-13	68·22	17·17	0·63	14·02	$Dy_{0.48}Si_{9.258}Al_{2.665}O_{1.180}N_{14.702}$	0·751
Yb System						
Sample	Si_3N_4	*AlN*	Al_2O_3	Yb_2O_3	*Overall formula*	k
AYb02	87·2	6·2	0	6·6	$Yb_{0.2}Si_{11.063}Al_{0.899}O_{0.795}N_{15.320}$	0·742
AYb025	84·26	7·64	0	8·1	$Yb_{0.25}Si_{10.888}Al_{1.129}O_{0.868}N_{15.318}$	0·742
AYb035	78·55	10·66	0	10·79	$Yb_{0.35}Si_{10.668}Al_{1.655}O_{1.021}N_{15.548}$	0·744
AYb04	75·8	12	0	12·2	$Yb_{0.4}Si_{10.405}Al_{1.883}O_{1.080}N_{15.431}$	0·744
AYb06	65·6	16·7	0	17·7	$Yb_{0.6}Si_{9.301}Al_{2.710}O_{1.362}N_{14.816}$	0·743
AYb07	60·87	18·98	0	20·15	$Yb_{0.7}Si_{8.853}Al_{3.156}O_{1.502}N_{14.659}$	0·743
AYb08	56·5	21·3	0	22·2	$Yb_{0.8}Si_{8.524}Al_{3.674}O_{1.650}N_{14.740}$	0·744
AYb10	48	25·2	0	26·8	$Yb_{1.0}Si_{7.499}Al_{4.501}O_{1.925}N_{14.216}$	0·743
AYb12	40·4	28·9	0	30·7	$Yb_{1.2}Si_{6.612}Al_{5.408}O_{2.208}N_{13.951}$	0·744
AYb02-13	79·72	10·68	3·03	6·61	$Yb_{0.2}Si_{10.099}Al_{1.550}O_{0.774}N_{14.700}$	0·753
AYb035-17	69·98	15·01	3·96	11·08	$Yb_{0.35}Si_{9.255}Al_{2.275}O_{0.981}N_{14.310}$	0·754
AYb035-13	73·05	14·19	1·71	11·09	$Yb_{0.35}Si_{9.652}Al_{2.146}O_{0.992}N_{14.705}$	0·752
AYb048-13	67·7	17·02	0·64	14·69	$Yb_{0.48}Si_{9.262}Al_{2.663}O_{1.180}N_{14.705}$	0·751
Y System						
Sample	Si_3N_4	*AlN*	Al_2O_3	Y_2O_3	*Overall formula*	k
AY033	82·89	10·94	0	6·17	$Y_{0.33}Si_{10.638}Al_{1.605}O_{0.988}N_{15.460}$	0·744
AY04	80·20	12·70	0	7·10	$Y_{0.4}Si_{10.841}Al_{1.963}O_{1.110}N_{16.078}$	0·745
AY048	76·13	15·10	0	8·77	$Y_{0.48}Si_{9.998}Al_{2.267}O_{1.201}N_{15.277}$	0·744
AY063	69·71	19·06	0	11·23	$Y_{0.63}Si_{9.383}Al_{2.933}O_{1.415}N_{15.131}$	0·744
AY08	62·68	23·53	0	14·33	$Y_{0.8}Si_{8.396}Al_{3.604}O_{1.643}N_{14.503}$	0·743
AY10	54·46	28·63	0	17·42	$Y_{1.0}Si_{7.501}Al_{4.509}O_{1.926}N_{14.227}$	0·744
AY02-13	82·04	10·99	3·12	3·90	$Y_{0.2}Si_{10.095}Al_{1.900}O_{1.30}N_{14.694}$	0·742
AY035-17	73·46	15·76	4·16	6·67	$Y_{0.35}Si_{9.249}Al_{2.752}O_{1.699}N_{14.302}$	0·750
AY035-13	76·68	14·90	1·78	6·67	$Y_{0.35}Si_{9.655}Al_{2.352}O_{1.299}N_{14.709}$	0·750
AY048-17	69·06	19·01	3·0	8·98	$Y_{0.48}Si_{8.857}Al_{3.143}O_{1.697}N_{14.301}$	0·750
AY048-13	72·22	18·16	0·69	8·98	$Y_{0.48}Si_{9.263}Al_{2.744}O_{1.301}N_{14.707}$	0·750

used as starting materials. The oxygen contents of the two nitride powders were taken into account when calculating the overall compositions. The overall compositions are given in Table 1. Compositions were chosen with reference to the extension of the Y-α-phase area as given by Sun *et al.*,[8] see Fig. 1(a). The α-sialon phase has an (Si,Al)/(O,N) ratio (k-value) of 0·75. Overall compositions which are more oxygen-rich than the α phase will have k values less than 0·75, while for compositions more rich in nitrogen k is > 0·75. As we have used M_2O_3 oxides as precursor materials, this implies that we could only obtain powder mixtures with k = 0·75 for compositions located on the oxygen-rich side of the join line Si_3N_4–M_2O_3 * 9 AlN. Samples with overall compositions along this line and those which are more nitrogen-rich have k values which are < 0·75, i.e. we are not able to fully compensate for the oxygen present on the surface of the nitrides, as seen in Table 1.

The starting materials, in batches of 30–50 g, were ball milled in water-free propanol for 24 h, using sialon milling media. After drying, compacted powders discs were hot-pressed (HPed) at 1800°C, at a pressure of 25–32 MPa, for 2 h in nitrogen in a graphite resistance furnace. The samples were allowed to cool inside the furnace by shutting off the power, yielding a cooling rate of ~50°C/min. The hot-pressed samples were then placed in a carbon crucible embedded in a mixture of Si_3N_4, AlN and BN packing powder and re-heated up to 1750°C in a standard graphite furnace in nitrogen atmosphere and equilibrated for 30 min, and then directly quenched (with a cooling rate of ~400°C/min) to room temperature. It has previously been noticed that the quenching procedure is essential in order to obtain true equilibrium conditions at the temperature of interest.[4–6]

The crystalline phases present in the prepared samples were determined from their X-ray powder diffraction patterns (XRD), obtained in a Guinier-Hägg camera with monochromatic Cu $K\alpha_1$ radiation. Small amounts of Si were used as internal standard, and the X-ray patterns were evaluated by means of the SCANPI system.[12] The unit cell parameters were refined with the PIRUM computer software.[13] The obtained unit cell parameters of the β-sialon phase, $Si_{6-z}Al_zO_zN_{8-z}$, were used to calculate its z value, using the equations given in Ref. 14. Polished surfaces of the prepared

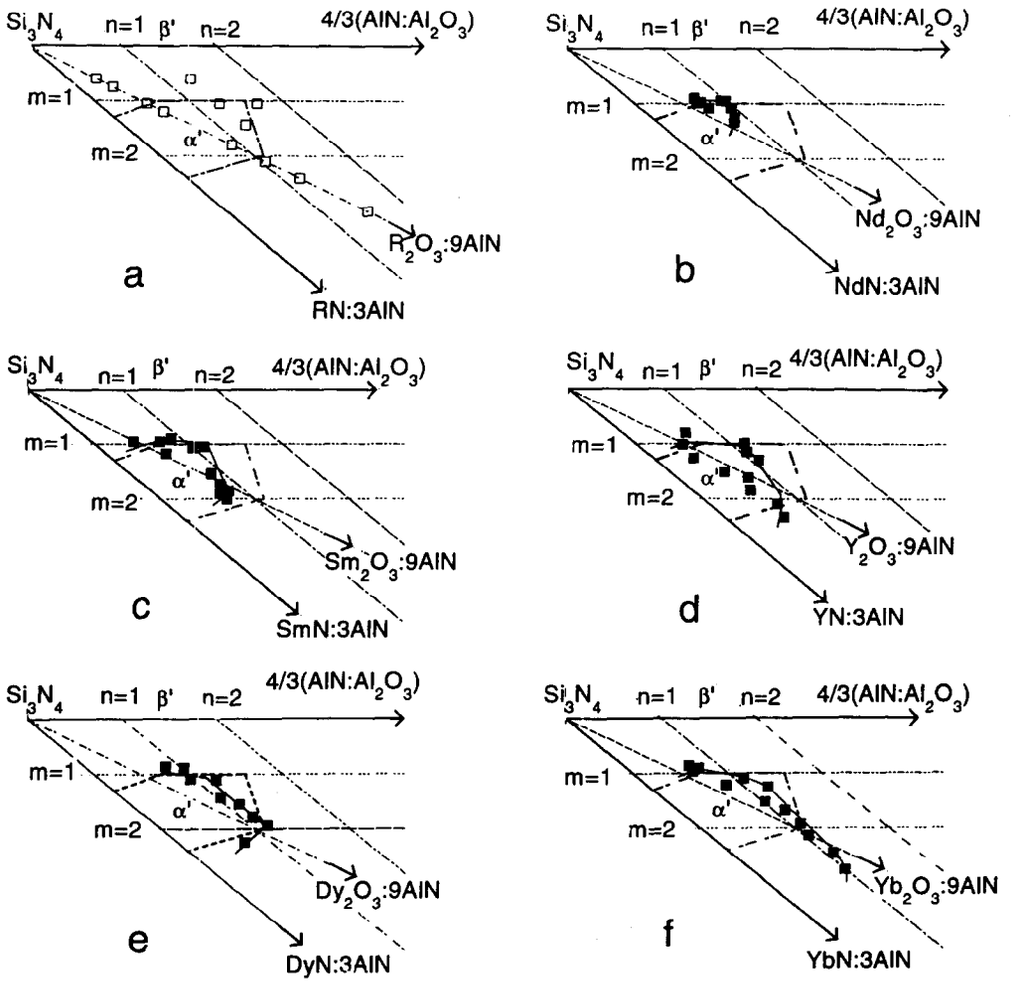

Fig. 1. The α-sialon region of the Y–α-sialon system according to Sun *et al.*[8] (a), the overall compositions of the prepared samples in this study are given by the symbol □. The extension of the α-sialon phase field in the M–α-sialon systems with M = (b) Nd, (d) Y, (e) Dy and (f) Yb. For comparison, the Sm system data given in Ref. 9 are reproduced in (c).

samples were examined in scanning electron microscopes (SEM, Jeol JSM 820) equipped with an energy dispersive spectrometer (EDS, Link AN 10 000). Calibration curves were used for quantitative EDS analysis of the compositions of individual α-sialon grains, β-sialon grains etc. The data given below are average values obtained from analyses of five or more grains for each phase in each composition. The errors in the determined m and n values are both estimated to be of the order $\pm$ 0·05.

3 Results and discussion

The unit cell parameters of the α- and β-sialon phases, the m, n and z values of the α and β phases and the Al/(Al + Si) ratio in the sialon polytype coexisting with the α and β phases in the samples prepared are given in Table 2. Using these m and n values, and assuming that all M ions in $M_xSi_{12-(m+n)}Al_{m+n}O_nN_{16-n}$ are trivalent, the boundaries of the α-sialon areas at 1750°C for M = Y, Yb, Dy, and Nd can be deduced and are depicted in Fig. 1. For comparison, corresponding data for the Sm system (given in Ref. 9) are included. Based on these data the following conclusions can be made:

(1) The α phase area becomes larger with decreasing size of the M ion, i.e. in the order Nd (0·99 Å) < Sm (0·96 Å) < Dy (0·91 Å) < Y(0·89 Å) < Yb (0·87 Å).

(2) The m_{min} values of the α-sialon phases formed in all systems studied are basically the same, i.e. $m_{min} \approx 1{\cdot}0$; the m_{max} values, however, show a tendency to increase with decreasing size of the M ion.

(3) The n_{max} value is 1·0 in the Nd system and around 1·2 in all other systems studied.

(4) The Yb system has the largest α-sialon area. However, recent studies have shown that the α-sialon phase in this system contains Yb^{3+} as well as Yb^{2+} ions.[15] The amount of Yb^{2+} present in the samples could not be determined but is anyhow expected to vary with the temperature and preparation conditions used. The n value of the Yb-α-sialon phase will increase with increasing Yb^{2+} content, and m will decrease, implying. that the most oxygen-rich α-sialon phase, the highest n_{max} value, is found in the Yb-α-sialon system.

(5) The β-sialon z values obtained from SEM-EDS analysis of individual β-grains and those calculated from XRD data are in fair agreement.

(6) The Al/(Al+Si) ratio of the sialon polytype coexisting with the α- and/or β-sialon phase(s) is very similar in the Y, Dy and Nd systems, viz. $\approx$ 0·8, while in the Yb-system the ratio is ~0·70.

These observations are in agreement with findings by Huang *et al.*,[3] who noticed that m_{max} ranged from 1·8 to 3·0 whereas all the m_{min} values were around 1·0 in samples with overall compositions along the join line Si_3N_4–M_2O_3 * 9 AlN and M = Y, Yb, Sm, and Nd. Our studies seem to confirm that the n_{max} value in the Y-α-sialon system is around 1·2. The observation that the Al/(Al+Si) ratio in the sialon polytype formed in conjunction with the α- and/or β-sialon phase(s) is lower ($\approx$ 0·70) in the Yb-sialon system than in the other systems studied ($\approx$ 0·80) suggests that the Al content in the intergranular phase is higher in the Yb-sialon system than in the other systems.

The lattice parameters of the hexagonal unit cell of α-sialon phase increase with increasing m and n values, while c/a ratio remains constant (0·728–0·729) as seen in Table 2.

Hampshire *et al.*[10,11] have derived empirical relationships between the cell dimensions of α-sialon and the overall composition of the sample, reading:

$$a(\text{Å}) = 7{\cdot}706 + 0{\cdot}0117\, m + 0{\cdot}824\, r_M + 0{\cdot}055\, x \quad (1)$$

$$c(\text{Å}) = 5{\cdot}578 + 0{\cdot}0259\, m + 0{\cdot}774\, r_M + 0{\cdot}0171\, n \quad (2)$$

where r_M is the radius of the M ion. Using the m, n and x values given in Table 2 as well as appropriate r_M values we have calculated the unit cell parameters and plotted these versus the observed ones in Figs 2 a(A) and b(A).

Sun *et al.*[8] have suggested a different relationship, which neglects the contribution from the M ions and reads:

$$a(\text{Å}) = 7{\cdot}752 + 0{\cdot}045\, m + 0{\cdot}009\, n \quad (3)$$

$$c(\text{Å}) = 5{\cdot}620 + 0{\cdot}048\, m + 0{\cdot}009\, n \quad (4)$$

The cell parameters thus predicted are plotted versus the observed ones in Figs 2 a(B) and b(B).

Figure 2 reveals that the relationship given by Sun *et al.* fits our data better than the one suggested by Hampshire *et al.* The data points of Fig. 2a(B) are scattered around the straight line representing a 1:1 relation between the predicted and measured a-axis. Furthermore, there seems to be no systematic variation in the data given in Fig. 2a(B) with respect to the size of the M ion, suggesting that the size of the lattice parameter does not depend on the size of the M ion or at least that such a dependence must be very small. The relationships computed by Hampshire and

Sun were mostly obtained from the m and n values of the starting compositions. Using m and n values based on our own analyses of individual α-sialon grains, we arrive at the following relationships (see Figs 2 a(C) and b(C)):

$$a(\text{Å}) = 7{\cdot}752 + 0{\cdot}036\,m + 0{\cdot}02\,n \quad (5)$$

$$c(\text{Å}) = 5{\cdot}620 + 0{\cdot}031\,m + 0{\cdot}04\,n \quad (6)$$

which deviate somewhat from the ones derived by Sun *et al.*

Table 2. Composition (m, n and z values) and lattice parameters of the α- and β-sialon phases, Al/(Al+Si) ratio in the polytype sialon phase *cf.* text

Sample	*Cell dimensions (Å)*						*EDS results*			
	α			β			α		β	*21R*
	a	b	c/a	a	c	z	m	n	z	Al/(Al+Si)
Nd System										
ANd02	7·793	5·667	0·727	7·616	2·916	0·40				
ANd035	7·805	5·679	0·728	7·616	2·917	0·41	1·0	0·66	0·45	0·82
ANd04	7·807	5·683	0·728				0·97	0·71		0·87
ANd06	7·827	5·701	0·728				1·34	0·81		0·80
ANd07	7·818	5·694	0·728				1·08	0·96		0·80
ANd08	7·816	5·693	0·728				1·08	0·96		0·79
ANd02-13	7·807	5·686	0·728	7·620	2·919	0·52	0·9	0·7		
ANd35-17	7·811	5·689	0·728	7·620	2·920	0·52	0·95	1·0		0·81
ANd35-13	7·811	5·689	0·728				1·09	0·72		0·79
ANd48-13	7·823	5·699	0·728				1·26	0·88		0·87
Dy System										
ADy02	7·789	5·665	0·727	7·615	2·915	0·36				
ADy025	7·793	5·669	0·727	7·616	2·917	0·41				
ADy035	7·798	5·676	0·278				0·86	0·84		
ADy04	7·807	5·687	0·728							
ADy06	7·832	5·713	0·729				1·55	1·15		0·77
ADy07	7·843	5·721	0·729				1·79	1·13		0·80
ADy08	7·850	5·726	0·729				1·94	1·18		0·83
ADy10	7·860	5·732	0·729				2·24	0·72		0·84
ADy02-13	7·803	5·685	0·729	7·626	2·924	0·71	0·88	1·03		
ADy35-17	7·817	5·699	0·729				1·10	1·23		
ADy35-13	7·814	5·695	0·729				1·09	0·95		
ADy48-13	7·826	5·707	0·729				1·42	1·04		
Yb System										
AYb02	7·788	5·662	0·727	7·616	2·916	0·40	0·91	0·64	0·43	
AYb025	7·791	5·665	0·727	7·616	2·917	0·41				
AYb035	7·799	5·675	0·728				0·86	0·69		
AYb04	7·806	5·682	0·728				0·96	0·66		
AYb06	7·832	5·708	0·729				1·68	1·14		
AYb07	7·842	5·716	0·729							
AYb08	7·848	5·721	0·729				2·14	1·06		0·72
AYb10	7·862	5·730	0·729				2·46	1·09		0·69
AYb12	7·872	5·736	0·729				2·76	1·0		0·71
AYb02-13	7·802	5·683	0·728	7·626	2·924	0·71	1·21	0·83		
AYb35-17	7·817	5·697	0·729				1·24	1·25		0·65
AYb35-13	7·810	5·689	0·728				1·09	1·10		0·67
AYb48-13	7·824	5·703	0·729				1·52	1·03		0·61
Y System										
AY033	7·801	5·679	0·728				1·0	0·49		
AY04	7·801	5·681	0·728				1·26	0·44		
AY048	7·818	5·696	0·729				1·51	0·58		
AY063	7·829	5·708	0·729				1·86	0·61		0·80
AY08	7·847	5·718	0·729				2·09	0·74		0·87
AY10	7·846	5·720	0·729				2·33	0·63		0·87
AY02-13	7·801	5·680	0·728	7·622	2·922	0·60				
AY035-17	7·813	5·694	0·729				0·99	1·17		0·79
AY035-13	7·813	5·698	0·729				1·15	1·07		0·77
AY048-17	7·823	5·703	0·729				1·62	0·75		0·80
AY048-13	7·825	5·702	0·729				1·31	1·09		0·78

The conclusion that the increase in unit cell dimensions of α-sialon is mainly due to an increase of the m value, i.e. to the replacement of (Si–N) by (Al–N), can be understood in terms of the fact that the average Al–N bond (1·87 Å) is much longer than an Si–N bond (1·74 Å). One must keep in mind that the Al–O and Si–N bond lengths are about equal (≈1·75 Å). Furthermore, the absence of any additional X-ray diffraction peaks indicates a random replacement of (Si–N) units by (Al–N) and (Al–O) units in the α-sialon structure.

For stoichiometric reasons, the amount of M ions present in the α phase is always related to the m value by the relation $x = m/3$. The data given above suggested, however, that size of the M ions has no or only a minor effect on the lattice expansion. The latter observation has been attributed to the size of M ions (r_M = 0·87–0·99 Å) being much less than the mean size of the interstitial hole (r = 2·59 Å) where they reside.[16,17] However, this argument is somewhat dubious, because it is well known that rare earth elements with ionic radii exceeding ~1 Å cannot be accommodated within the α-sialon structure. This point will be discussed in some detail in a forthcoming article.

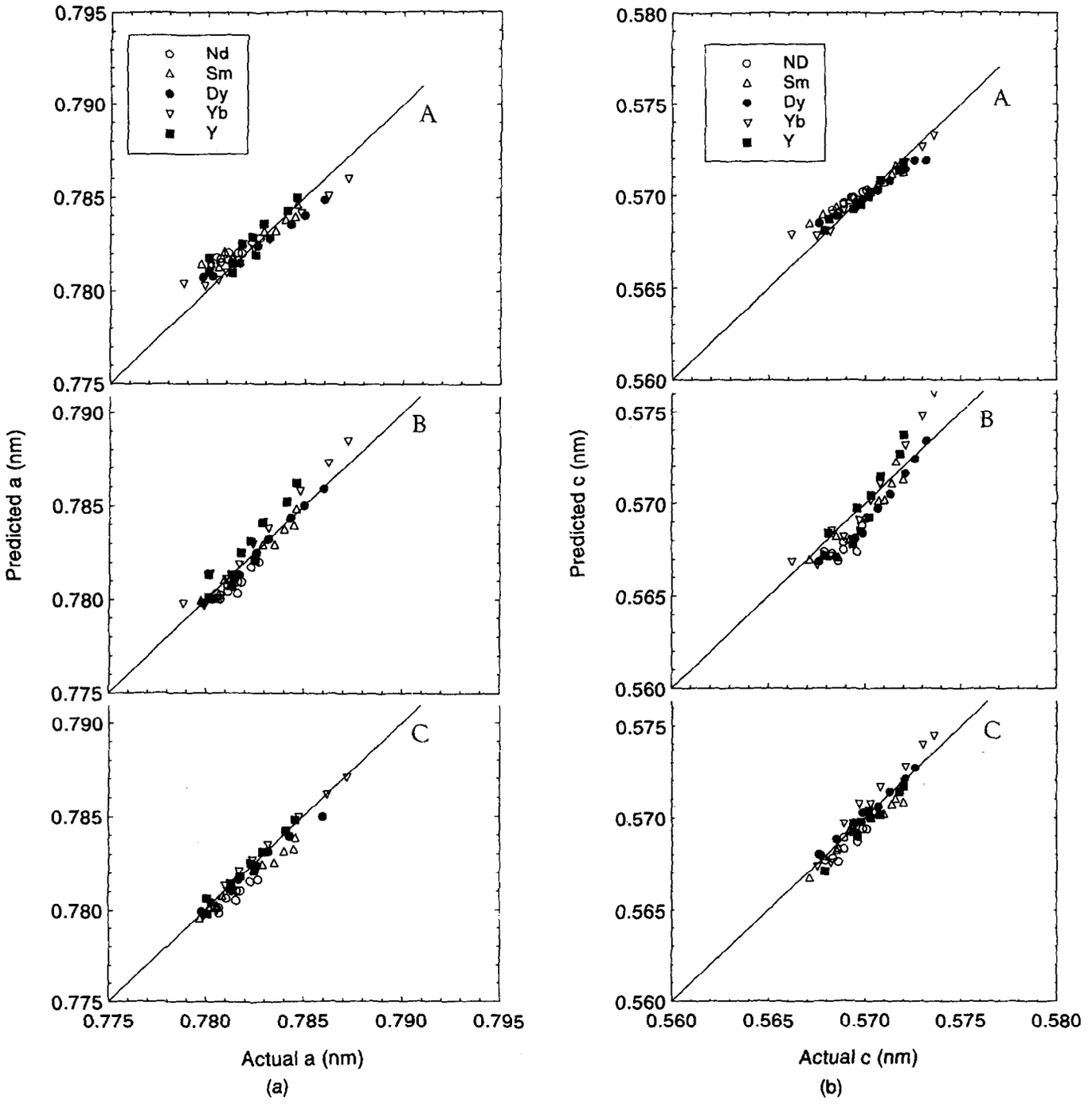

Fig. 2. Predicted unit cell dimensions (a) a and (b) c, using the relationships deduced by Hampshire *et al.* (A), by Sun *et al.* (B) and based on our data (C) plotted versus observed lattice parameters.

Acknowledgements

Prof. T. Ekström's valuable comments are gratefully acknowledged and so is the financial support by the Swedish Research Council for Engineering Science.

References

1. Sun, W. Y., Tien, T. Y. and Yen, T.-S., Subsolidus phase relationships in part of the system Si, Al, Y/N, O: The system Si_3N_4–AlN–YN–Al_2O_3–Y_2O_3. *J. Am. Ceram. Soc.*, 1991, **74**, 2753–2758.
2. Sun, W. Y., Yen, D. S., Gao, L., Mandal, H., Liddell, K. and Thompson, D. P., Subsolidus phase relationships in Ln_2O_3–Si_3N_4–AlN–Al_2O_3 (Ln = Nd, Sm). *J. Eur. Ceram. Soc.*, 1995, **15**, 349–355.
3. Huang, Z. K., Tien, T. Y. and Yen, T. S., Subsolidus phase relationships in Si_3N_4–AlN–Rare earth oxide systems. *J. Am. Ceram. Soc.*, 1986, **69**, C-241–C-242.
4. Shen, Z., Ekström, T. and Nygren, M., Ytterbium stabilised α-sialon ceramics. *J. Phys. D: Appl. Phys.*, 1996, **29**, 893–904.
5. Shen, Z., Ekström, T. and Nygren, M., Homogeneity region and thermal stability of neodymium doped α-sialon ceramics. *J. Am. Ceram. Soc.*, 1996, **79**, 721–732.
6. Shen, Z., Ekström, T. and Nygren, M., Preparation and properties of stable dysprosium doped α-sialon ceramics. *J. Mater. Sci.*, 1997, **32**, 1325–1332.
7. Stutz, D., Greil, P. and Petzow, G., Two-dimensional solid-solution formation of Y-containing α-Si_3N_4. *J. Mater. Sci. Lett.*, 1986, **5**, 335–336.
8. Sun, W. Y., Tien, T. Y. and Yen, T.-S., Solubility limits of α′-sialon solid solutions in the system Si, Al, Y/N, O. *J. Am. Ceram. Soc.*, 1991, **74**, 2547–2550.
9. Nordberg, L.-O., Shen, Z., Nygren, M. and Ekström, T., On the extension of α-sialon solid solution range and anisotropic grain growth in Sm-doped α-sialon ceramics. *J. Eur. Ceram. Soc.*, 1997, **17**, 1575–1580.
10. Hampshire, S., Park, H. K., Thompson, D. P. and Jack, K. H., α′-Sialon ceramics. *Nature (London)*, 1978, **274**, 880–882.
11. Redington, M., O'Reilly, K. and Hampshire, S., On the relationships between composition and cell dimensions in α-sialons. *J. Mater. Lett.*, 1991, **10**, 1228–1231.
12. Johansson, K.-E., Palm, T. and Werner, P.-E., An automatic microdensitometer for X-ray powder diffraction photographs. *J. Phys.*, 1980, **E13**, 1289–1291.
13. Werner, P.-E., A Fortran program for least-squares refinement of crystal structure cell dimension. *Arkiv för Kemi*, 1969, **31**(43), 513.
14. Ekström, T., Käll, P.-O., Nygren, M. and Olsson, P.-O., Single-phase β-sialon ceramics by glass-encapsulated hot isostatic pressing. *J. Mater. Sci.*, 1989, **24**, 1853–1861.
15. Shen, Z., Nygren, M. and Hålenius, U., Absorption spectra of rare-earth doped α-sialon ceramics. *J. Mater. Sci. Lett.*, 1997, **16**, 263–266.
16. Cao, G. Z. and Metselaar, R., α-Sialon Ceramics: A review. *Chem. Mater.*, 1991, **3**, 242–252.
17. Izumi, F., Mitomo, M. and Suzuki, J., Structure refinement of yttrium α-sialon from X-ray powder profile data. *J. Mater. Sci. Lett.*, 1982, **1**, 533–535.